26 May 2010, 4:45 pm - 6:45 pm

Large Scale Model Test for Pile-Supported Wharf in Liquefied Sand

Wen-Jong Chang
National Cheng Kung University, Taiwan

Jyh-Fang Chen
Institute of Transportation, Taiwan

Hsing-Chuan Ho
Sinotech Engineering Consultants, Taiwan


Fifth International Conference on
Recent Advances in Geotechnical Earthquake Engineering and Soil Dynamics
and Symposium in Honor of Professor I.M. Idriss
May 24-29, 2010 • San Diego, California

LARGE SCALE MODEL TEST FOR PILE-SUPPORTED WHARF IN LIQUEFIED SAND

Wen-Jong Chang
National Cheng Kung University
Tainan, Taiwan 70101

Jyh-Fang Chen
Harbor and Marine Technology Center, Institute of Transportation,
Taichung, Taiwan 435

Hsing-Chuan Ho
Geotechnical Engineering Research Center, Sinotech Engineering Consultants,
Taipei, Taiwan 11071

ABSTRACT

Pile-supported wharf is a general option in port design to provide lateral resistance and bearing capacity under both static and dynamic loadings. In situ large-scale physical modeling using surface wave generator was performed to study the dynamic soil-structure interactions in pile-supported wharves and to serve as a prototype for in situ monitoring station. A wharf model consisting of 2 steel pipe piles welded on a steel slab was installed on a reconstituted underwater embankment. Due to screening of stress wave, the two piles are subjected to different loading conditions. Data reduction procedures were developed to analyze coupled shear strain-pore pressure generation behavior, pile responses, and soil-pile interaction characteristics. The results proved that the physical modeling can capture the interactions among the induced shear strain, generated excess pore pressure, and dynamic *p-y* behavior around piles. Preliminary results also show that evolutions of dynamic *p-y* curve with excess pore pressure variations should be included in soil-pile interaction modeling.

INTRODUCTION

Soil liquefaction is the most widespread seismic damage to port and harbor facilities because native soils or hydraulic fills in ports are generally loose, saturated, cohesiveless soils. Pile-supported wharves, consisting of a soil or rock underwater embankment, a rigid deck above the embankment, and piles connected to the deck, are common waterfront facilities providing lateral resistance and bearing capacity under both static and dynamic loadings. Pile-supported wharf failures in liquefied soils had been found at the port of Oakland during the 1989 Loma Prieta Earthquake (Werner 1998) and Takahama in Kobe during the 1995 Hyogo-ken Nambu Earthquake (Tokimatsu and Asaka 1998). Previous studies reveal that forces applied on wharf piles during seismic loading can be divided into inertial forces induced by vibrations of superstructure and kinematic forces from the relative deformations of surrounding soil. However, evaluations of inertial and kinematic effects in soil-pile systems involve highly complicated soil-pile-structure interaction mechanism, which remains a highly challenging issue in geotechnical earthquake engineering field.

Techniques for analyzing soil-pile interaction in liquefiable sandy soils can be categorized into four branches: pseudo-static analyses (e.g., Rollins et al. 2005), dynamic numerical simulations (e.g., Boulanger et al. 1999), laboratory physical modeling (e.g., Brandenberg et al. 2005), and in situ dynamic testing (e.g., Kamaji et al. 2005). The complexity of the mechanism and knowledge involved makes these numerical simulations require rigorous verifications. To improve the applicability of pseudo-static approaches and verify numerical results, large-scale physical modeling and long waiting field monitoring stations are required.

Many insights of soil-pile interaction behaviors come from observations and interpretations of laboratory physical modeling. Techniques used in this category include 1g-shaking table tests (Tokimatsu and Suzuki 2004) and centrifuge tests (Brandenberg et al. 2005). However, due to the complexity of in situ soil stratum, nonlinear soil responses, and disturbance from pile installation, in situ dynamic soil-pile interaction testing is preferred and sometimes the only option in evaluating the site specific liquefaction responses of pile-support wharves. Rollins et al. (2005) and Kamaji et al. (2005)

used controlled blasting to induce soil liquefaction in the field and observed the soil and pile responses. Due to the damage from blasting, this type of technique is not suitable for active facilities. Alternatively, installation of a long waiting instrumentation on active wharves for future seismic events and development of testing techniques that can directly measure the soil-pile-structure interactions under controlled loading are warranted.

This paper presents a pilot test which implemented the in situ dynamic liquefaction test proposed by Rathje et al. (2005) on a wharf model in liquefiable soil. The test aimed to: (1) verify configuration of in situ seismic monitoring stations on active wharf facilities, (2) develop technique for integrity check of the in situ instrumentation system, and (3) perform seismic soil-structure interaction study on pile-supported wharves. A vibroseis truck, which is a mobile servo-hydraulic shaker mounted on a transport vehicle, was used to generate surface waves propagating laterally to a large scale wharf model. The dynamic source produced a uniform stress profile laterally applied on middle section of the pile, which is useful in studying the BNWF behaviors around piles. Instrumentation was configured to measure dynamic soil motions, pore pressure variations and pile responses. Data reduction procedure was developed to extract nonlinear soil properties, coupled shear strain-pore pressure response, pile responses and soil-pile interactions.

TESTING METHODOLOGY

Analyses of pile-supported wharves on liquefiable soil require studying of dynamic behavior of pile system, nonlinear soil responses with pore pressure generation, and soil-pile-superstructure interactions. The in situ model test involves dynamically loading wharf model in the field while simultaneously measuring the soil and wharf model responses. To account for different loading modes between the real earthquake excitations due to upward propagating shear waves and the laterally propagating surface waves in proposed test, soil responses are analyzed on shear strain basis instead of soil motion quantities such as acceleration or velocity. Configured instrumentation was used to evaluate induced shear strains, pore pressure variations, wharf responses, and soil-pile interactions.

Testing Layout and Dynamic Source

Testing components of the dynamic wharf model test include a surface dynamic loading system, a wharf model on liquefiable underwater embankment, and configured instrumentation. Testing layout and configuration of the in situ wharf modeling is shown in Figs. 1 and 2. The testing site is a reclaimed land in Taichung harbor, Taiwan. The native soil profile is characterized by boring and seismic survey. The top 4 m of field soil is backfilled crust with USCS classification of SM and the average shear wave velocity of this layer is 200 m/s. The soil below the crust is hydraulic filled silty sand classified as SM with shear wave velocity from 200 to 310 m/s. The ground water table varies with tides and within depths of 3.5 to 5.0 m.

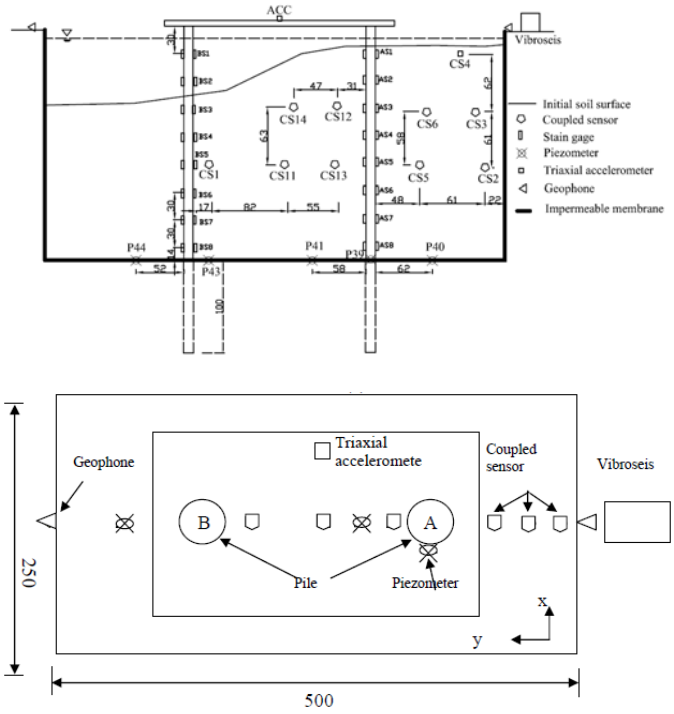

Fig. 1. Layout of wharf model test (unit: cm).

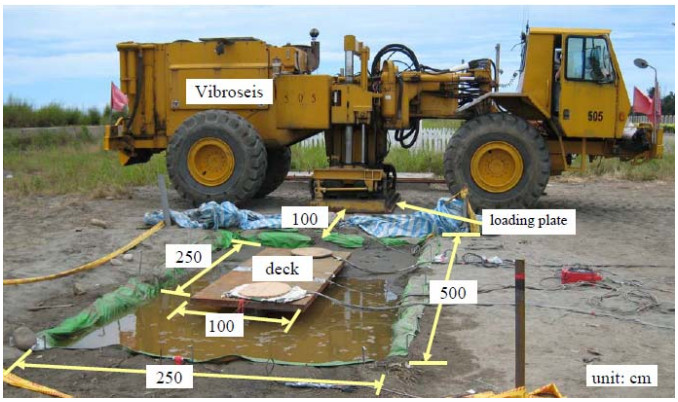

Fig. 2. Vibroseis truck and setup of wharf model test

The surface dynamic loading source consists of a vibroseis truck and a rectangular loading plate. The vibroseis truck served as a vertical vibration source that dynamically loaded the rectangular steel plate on the ground surface. The loading plate is placed 1 m from the tested model and lined up on the center line of the model for symmetric consideration. The symmetric alignment between the dynamic source and the model reduced the three-dimensional conditions to a two-dimensional plane wave configuration. The vibroseis truck (Fig. 2) used in this test can generate sinusoidal waves with a frequency range of 7-100 Hz, maximum amplitude of 225 kN, and duration up to 30 sec. Similar system used by Rathje et al.

(2005) had proven that the generated surface waves is capable of inducing shear strain amplitude greater than the general threshold shear strain level (~10^{-2}%) and generating significant excess pore pressure.

Preparation of wharf model

A model wharf consisting of two steel pipe piles with pile heads welded on a steel plate was installed on a reconstituted underwater embankment to represent a pile-supported wharf on liquefiable soil. The dimensions of deck plate are 250 by 100 by 1 cm with respect to length, width, and thickness. Each steel pipe pile is 350 cm long with a 20 cm outer diameter and 0.5 cm thickness. The bottom 100 cm of piles was pushed into the native soil statically after trench excavation and the remained 250 cm was buried by the reconstituted soil. After the driving of piles, the deck plate was welded on top of piles as rigid connections and the horizontal distance between the two piles was 190 cm from center to center.

To produce uniform, saturated soil stratum, the reconstituted underwater embankment was prepared by water sedimentation. The reconstituted soil was divided into seabed, underwater slope, and level backfill. The seabed and the level backfill were constructed from two ends of the trench and the underwater slope was formed in the natural rest angle of soil. A test trench with dimensions of 5.0 by 2.5 by 2.5 m with respect to length, width and depth respectively was excavated. Because native ground water table is below 3 m, a thin, impermeable membrane was placed on the excavated surface to prevent water leakage from the trench and maintain the saturation of the reconstituted soil. Soil borrowed from the nearby beach was used to prepare the underwater embankment. The borrowed soil is a non-plastic, clean, fine sand classified as SM soil in USCS classification with a specific gravity of 2.66. Post-test borings confirmed that the spatial variations of void ratio and unit weight were small, indicating that the reconstituted soil was quite uniform. The reconstituted soil has an initial void ratio of 0.94 and saturated unit weight of 18.1 kN/m^3. Bender element tests on reconstituted specimens showed that the shear wave velocity at 1.25 m deep was 80 m/s and the value was checked by travel time of wave propagation in the level backfill. This shear wave velocity corresponds to a normalized shear wave velocity (V_{s1}) of 156 m/s, which will liquefy under small cyclic stress ratio (~0.1) for earthquakes of magnitude 7.5.

Instrumentation

To simultaneously monitor soil motions and pore pressure variations, the “coupled sensor” was fabricated by integrating a triaxial, low-frequency accelerometer and a miniature pore pressure transducer in an cylindrical, acrylic case of a size of 55 mm in diameter and 78 mm in length. A triaxial capacitive accelerometer was used for measuring the local ground accelerations in the vertical and two orthogonally horizontal directions. Eight coupled sensors were deployed, as shown in Fig. 1, to form two 0.6 by 0.6 m square arrays on the vertical plane along the center line of the trench. Other embedded sensors include one coupled sensor placed near the top of the level backfill, another one in front of Pile B, and five piezometers (P39, 40, 41, 43, and 44) at the bottom of the test pit.

Pile responses were monitored by strain gage pairs glued on opposite sides of a pile with 30 cm vertical interval to measure the induced bending strain profiles. Advantages of this type of strain gage layout include temperature compensation, cancelation of thermal effect of lead wires, removal of axial strain, and double magnitude of output voltages. Using an elastic beam theorem with proper end conditions, profiles of moment distribution, lateral displacement, and subgrade reaction on piles can be evaluated. Deck plate motion was measured by a triaxial accelerometer and used to verify the evaluated lateral displacements of piles.

All the embedded sensors were installed before the water sedimentation process. Piezometers and coupled sensors were fixed at the designated locations with proper orientations by fishing lines after excavation. All fishing lines were cut prior to shaking test to make sensors move with the soil. A customized, stand-alone dynamic data acquisition system was used for these sensors. In the performed tests, data acquired from accelerometers and piezometers were collected at a sampling rate of 1000 Hz for better resolution in wave velocity determination by travel time interval and smoother integration for soil displacement and velocity calculations. Piezometer data were continuously recorded after shaking to capture the dissipation process of the excess pore pressures. Down-sampling technique was adopted in data processing to reduce data points of pore pressure time histories.

Testing procedure

A total of 15 test events were conducted to study the effects of loading amplitude, frequency, and soil properties on soil-pile interactions. Several small amplitude tests were performed for system check and wave velocity measurements. After each test event, surface survey was conducted to monitor the surface variations and induced settlements.

DATA ANALYSIS

Data collected from the embedded instrumentation include histories of particle motion, pore pressure, pile bending strain, and deck acceleration. These data were processed and analyzed to evaluate the temporal and spatial variations of shear strain and excess pore pressure induced in the embankment, horizontal pile deformations, subgrade reactions, and nonlinear soil-pile interactions. The data reduction procedure is show in Fig. 3 and details are described below.

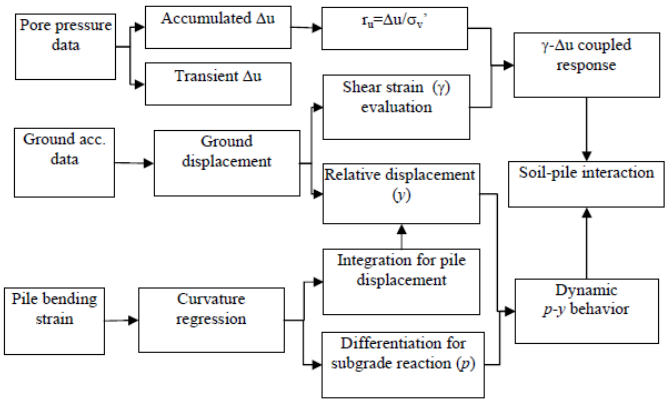

Fig. 3. Data reduction procedure

Shear strain evaluation

To be comparable with real seismic excitations mainly due to upward propagating shear waves, soil responses were represented in terms of induced shear strain instead of soil particle motion quantities. The testing configuration was setup in a plane wave condition and only the shear strains on the vertical plane of the center line needed be considered. Validations of the plane wave condition were confirmed from small soil motions in the direction normal to the vertical plane (x-direction in Fig. 1(a)).

To calculate the induced shear strains under the complicated wave field, the 2D displacement-based method (denoted as 2DBM) described in Rathje et al. (2005) was implemented. The instrumentation array formed by four coupled sensors is considered as a 4-node element with 2 degrees of freedoms (vertical and horizontal) per node. The vertical and horizontal directions are parallel to the particle motion direction (i.e., z- or y-direction) respectively. Taking the instrument array within the level backfill (CS2, 5, 6, and 3) as an example and assuming that the element size in Fig. 1(a) is approximately 2a in both y (horizontal) and z (vertical) directions and the origin (y=0, z=0) of the element is at the center of the array, the coordinates of the four coupled sensors are $(-a,-a)$, $(a,-a)$, (a,a), and $(-a,a)$ for CS2, CS5, CS6, and CS3 respectively. On yz-plane, the shear strain at any point within the array with coordinates (y, z), γ_{yz}, is evaluated by:

$$\gamma_{yz}(y,z)=\frac{1}{4a}\left[-u_{y2}(1-\frac{y}{a})-u_{z2}(1-\frac{z}{a})-u_{y5}(1+\frac{y}{a})+u_{z5}(1-\frac{z}{a})\right.$$
$$\left.+u_{y6}(1+\frac{y}{a})+u_{z6}(1+\frac{z}{a})+u_{y3}(1-\frac{y}{a})-u_{z3}(1+\frac{z}{a})\right] \quad (1)$$

where u_{ij} is the displacement in the i direction (i = y or z) at node j (j = CS2, 5, 6 and 3). The nodal displacements are computed by double integration on the vertical and horizontal acceleration histories with baseline corrections applied to remove the drifts by noises. To evaluate the coupled shear strain-pore pressure response at locations of coupled sensors, shear strains at the locations of coupled sensors needed be evaluated. For example, the shear strain at CS5 (i.e, y=a, z=-a) is evaluated by:

$$\gamma_{yz}(y=a,z=-a)=\frac{1}{2a}\left[-u_{y5}+u_{z5}-u_{z2}+u_{y6}\right] \quad (2)$$

where a=30 cm with displacement unit of cm.

Excess pore pressure ratio

The recorded pore pressures contained three components: (a) the hydrostatic pore pressure of the ground water table, (b) the transient excess pore pressure oscillating with the dynamic loading, and (c) the accumulated excess pore pressure (Δu) representing the net outcome between the accumulation and dissipation of the excess pore pressure. To focus on excess pore pressures, hydrostatic pore pressures were subtracted from the records. To highlight and analyze the transient and accumulated excess pore pressures separately, band-passing and low-passing filters are used respectively. To calculate the excess pore pressure ratio ($r_u=\Delta u/\sigma_{vo}^{'}$), defined as the accumulated excess pore pressure (Δu) normalized to the initial vertical effective stress ($\sigma_{vo}^{'}$), the initial vertical effective stress was inferred from the submerged unit weight of soil ($\gamma'=\gamma_{sat}-\gamma_w$ =8.3 kN/m^3) and the depth of sensor. Initial liquefaction is defined as the state that the accumulated excess pore pressure reaches the initial vertical effective stress or r_u is a unity. Combining the computed shear strain at the location of pore pressure measurement, the coupled response of the shear strain and the excess pore pressure can be evaluated.

Pile behavior and soil-pile interaction

On a BWF framework, soil-pile interaction at a specific depth is described as:

$$EI\frac{\partial^4 y}{\partial z^4}=k\mathrm{D}(y_s-y) \quad (3)$$

where E and I are Young's modulus and moment inertia of the pile respectively, y is the lateral deflection of pile, y_s is horizontal displacement of soil, k is the modulus of horizontal subgrade reaction, and D is the pile diameter. For the steel model piles, E=2.1×10^{11} N/m^2, I=1.7×10^{-5} m^4, and D=0.2 m. Assuming that the beam behaves linearly and the cross section of the pile is uniform, the curvature (κ) of pile, bending stain (ε), and lateral deflection (y) at a depth of z is related by:

$$\kappa(z,t)=\frac{[\varepsilon_n(z,t)-\varepsilon_s(z,t)]}{D}=\frac{\partial^2 y(z,t)}{\partial z^2} \quad (4)$$

where ε_n and ε_s are bending strain on opposite side with distance of D in the direction normal to neutral plane. For

strain gage pairs on opposite sides, ε_s(z) is equal to $-\varepsilon_n$(z) and D is constant. With specified end conditions, the horizontal displacement of pile can be evaluated by:

$$y(z,t) = \iint \kappa(z,t)dzdz \tag{5}$$

The horizontal displacement of soil is evaluated from numerical double integration of acceleration data. The relative displacements between the pile and soil were evaluated accordingly.

The bending moment on the pile is:

$$M(z,t) = EI\frac{\partial^2 y(z,t)}{\partial z^2} = EI\kappa(z,t) \tag{6}$$

The net distributed horizontal stress (p) per unit length on the pile is:

$$q(z,t) = EI\frac{\partial^4 y(z,t)}{\partial z^4} = EI\frac{\partial^2 \kappa(z,t)}{\partial z^2} \tag{7}$$

The subgrade reaction of soil on pile, *p*, expressed as the net horizontal force of unit length, is calculated from:

$$p(z,t) = q(z,t) = kD \tag{8}$$

Combine the subgrade reaction from Eq. (7) and relative displacement between the pile and surrounding soil and, the *p-y* behavior was established.

Curve fitting functions with existence of second derivatives have been used to interpret lateral response of piles subjected to lateral loading. The cubic spline interpolation is used in this study with specified boundary conditions at both pile ends. Advantages of using cubic spline interpolation include: (1) passing every measured point smoothly, (2) avoidance of error accumulation with order of polynomials, (3) being applicable to limited data points, and (4) simplicity (Nakamura 1995). Because the top of the pile is welded on the steel deck and the deck move horizontally, zero curvature at the pile top is assumed. Although the pile is 3.5 m long, only the portion within the reconstituted soil (2.5 m) was measured and the bottom 1.0 m was penetrated in the native soil, which was neither liquefied nor subjected to large stiffness reduction due to small shear strain level. Therefore, a fixed portion of piles within the native soil is assumed. The curvature at the bottom of the test pit is linearly extrapolated from the lowest measuring point (0.14 m from bottom).

The fitted curvature curves were doubly integrated to compute the distribution of lateral displacement and differentiated twice to estimate the profile of subgrade reaction in every time step. To minimize the effects of noise on numerical calculations, band-passing filter, which retained components with 0.5 to 1.5 times of loading frequency, was applied on bending strain histories before numerical calculations. Verifications of end condition assumptions and filtering effects were conducted by comparing the pile head displacement amplitudes with the measured relative deck displacement amplitudes estimated from double integration of the deck acceleration subtracting the bottom displacement and the results are shown in Fig. 4. The average pile head amplitudes of the two piles, which take into account of the deformation of deck plate, agree well with the relative deck displacement amplitudes, indicating that the procedure for bending strain processing is adequate for displacement evaluation. Validation of subgrade reaction evaluation is more complicated. However, qualitative agreements in the observed soil-pile interactions provide certain degree of confidence on the evaluated results.

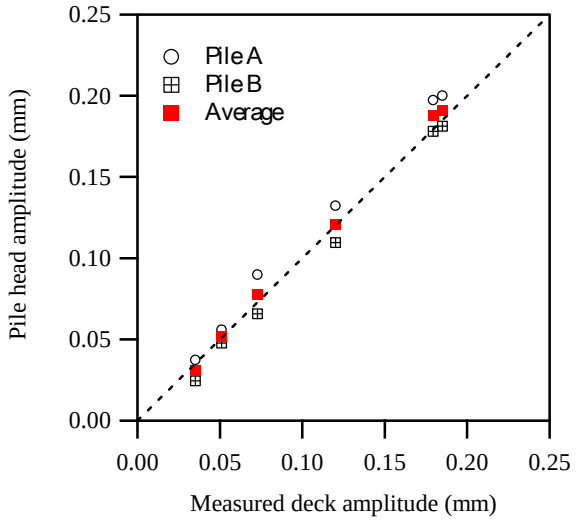

Fig. 4. Comparison of deck displacement amplitude

TYPICAL TESTING RESULTS

Results from event 9, which is the first test with liquefaction occurred in the entire embankment, are presented to show the wharf responses in liquefied sand.Data of the coupled shear strain-pore pressure response and the temporal and spatial variations of excess pore pressure are presented to demonstrate the liquefaction process. Dynamic p-y behaviour is evaluated from piles and adjacent soil responses to represent the dynamic soil-pile interactions.

Pore pressure variations

The accumulated excess pore pressure histories of event 9, processed by low-passing 1 Hz, are shown in Fig. 5 along with the time of initial liquefaction. Variations of excess pore pressure at level backfill and bottom of test pit are presented in group to demonstrate the liquefaction process of the embankment. The initial liquefaction was first observed at CS5 (Fig. 5(a)), where relatively large accelerations were

observed. After the initial liquefaction at CS5, initial liquefaction was observed on bottom of the embankment. The location of CS4 (0.4 m deep) was not liquefied due to the smaller induced shear strain and faster dissipation.

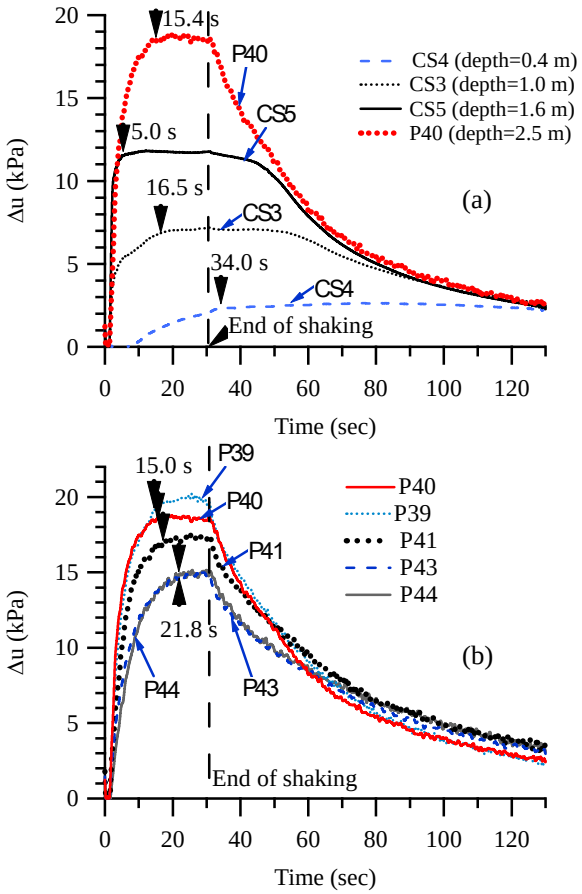

Fig. 5. Variation of accumulated excess pore pressure (low-passing 1 Hz) in liquefied case (event 9)

Time histories of excess pore pressures at the bottom of the test pit is shown in Fig. 6(b), which indicated that the initial liquefaction was first occurred near the piles and quickly extended laterally. Same trend was observed at the depth of 1.6 m, where initial liquefaction was observed in the sequence of CS5, CS13, and CS1. The temporal variations of liquefaction process indicated that the existence of pile affected the pore pressure accumulation and the rate of pore pressure accumulation decreases as the distance to the pile increases. Detail mechanism is better explained from the coupled strain-pore pressure response and pile behavior, which are presented in next section.

Soil coupled response

Spatial variations of soil acceleration histories are shown in Fig. 6. In Fig. 6 all the data are processed with band-passing filter of frequency between 7.5 to 22.5 Hz. The vertical and horizontal motion components within level backfill generally agree with the wave characteristics of Rayleigh waves, including retrograde elliptical particle traces, higher amplitude in vertical component except near surface, varied vertical amplitude with maximum value at the depth of 1/3 wave length (Woods 1968). However, the motion sensors at the slope recorded different motion pattern. The horizontal component of soil behind Pile A is very small except CS14, where the location was close to the sloping surface and the reflected waves from the sloping surface were recorded. The significant reduction in both horizontal and vertical motions behind the pile is the outcome of screening effects of stress waves due to the pile and the shear strain is significantly reduced, as shown in Fig. 8.

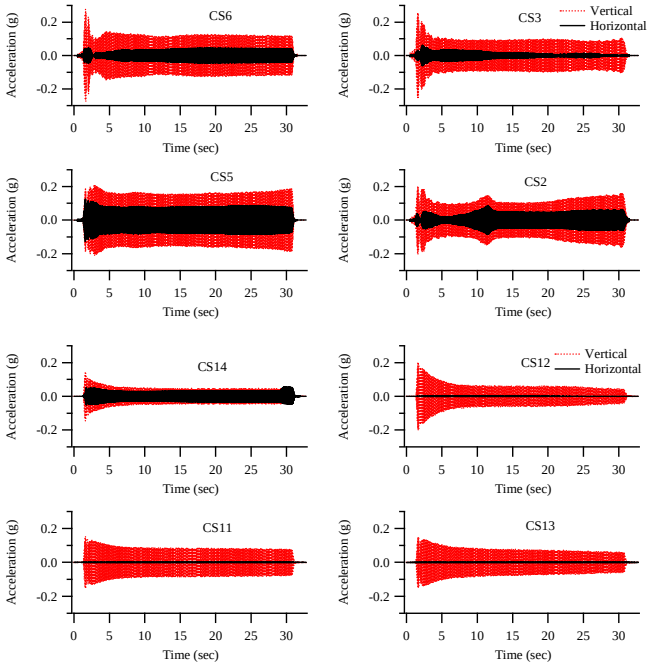

Fig. 6. Acceleration records for event 9

The induced shear strains at locations of CS5 and CS13 calculated by 2DBM are plotted along with the corresponding excess pore pressures in Fig. 7(a) and 7(b) respectively to show the coupled shear strain-pore pressure responses ahead and behind Pile A. The coupled shear strain-pore pressure response at CS5 agreed with a typical response of saturated sand in level free field in terms of deformation mode and pore pressure generation pattern. The coupled response behind Pile A showed significant reductions in shear strain due to screening of stress waves (Fig. 7(b)). Although the amplitude of shear strain at CS13 is at the margin of threshold shear strain, the generated excess pore pressure still reached initial liquefaction state later. Similarity among the pore pressure histories at the bottom and the nearby coupled sensor (CS13 vs. P41, and CS1 vs. P43) indicates that the excess pore pressures behind Pile A were not solely generated from induced shear strains but also affected by the hydraulic gradients among surrounding soils.

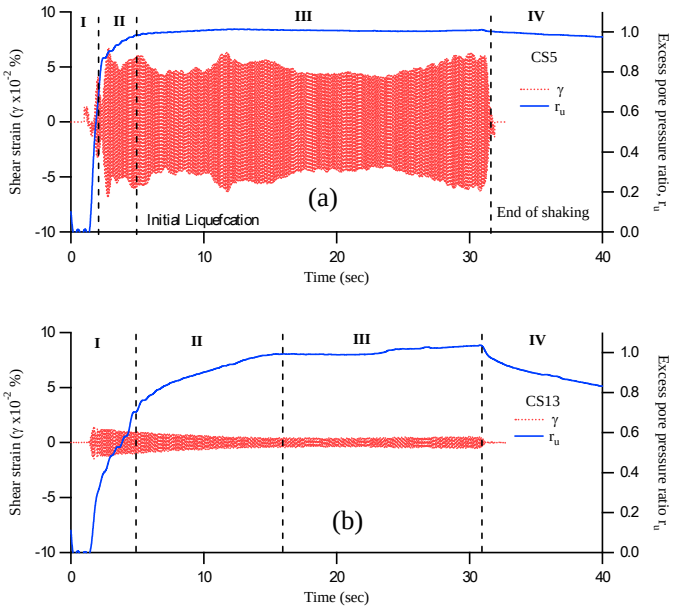

Fig. 7. Coupled shear strain-pore pressure response in liquefied case (event 9)

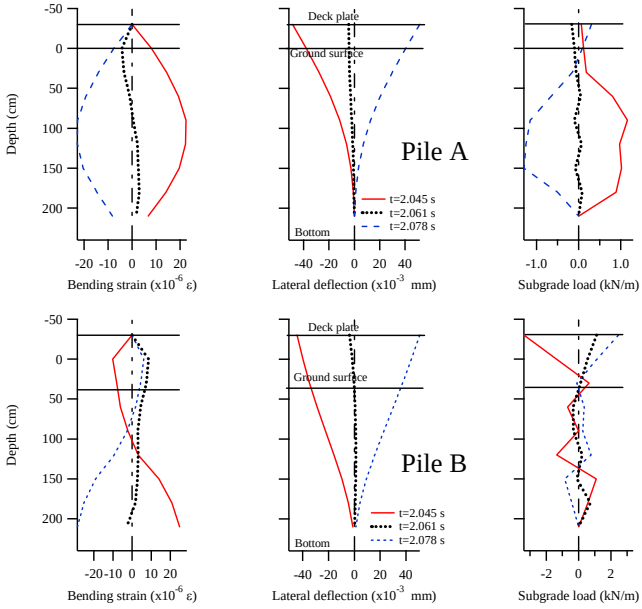

Fig. 8. Response profiles of piles in event 9

Dynamic soil-pile interaction

Profiles of bending strain, lateral deflection, and subgrade load of Pile A and Pile Bduring the largest response cycle in event 9 are shown in Figs. 8(a) and 8(b), respectively. The maximum bending strain/moment was observed at the middle of the pile (from 90 cm to 150 cm deep) then gradually decreased as the depth decreased. The displacement profiles show that the pile vibrated in the fundamental mode with fixed end near the bottom of the trench and zero curvature at the top. The subgrade load distributions shown in Fig. 8(a) indicate that a uniform subgrade pressure was applied at the middle section of the pile. The uniform lateral pressure section provides a better controlled condition in back-calculating the *p-y* response. Nevertheless, the results demonstrate that Pile A was mainly subjected to kinematic forces from surrounding soil due to stress wave propagation.

However, responses of Pile B at the same time steps are different although the pile head displacements are close, as shown in Fig. 8(b). The response profiles of Pile B indicate that Pile B was under a pushover condition with forced displacement on top in which the inertial forces is more dominating. The non-zero subgrade load above the ground surface is numerical error due to limited measurement points in cases of a point load on pile head. The cause of different loading condition of Pile B is the outcome of screening effects and rigid connections of piles on the deck plate. Although the current configuration induced two different loading mechanisms of piles on same deck plate, it provides a testing technique that can study the two loading conditions in one test and could represent pile groups subjected to inclined waves.

Figure 9 shows the dynamic *p-y* curves of Pile A at different depths with three excess pore pressure ratios calculated from adjacent pore pressure measurements in level backfill (P39, P40, CS5, and CS3). The hysteretic curve of p-y response is similar to the BNWF model proposed by Boulanger et al. (1999). These figures demonstrate that the dynamic *p-y* curves were significantly affected by the generated excess pore pressure ratio of surrounding soils. For clear demonstration, the evolution of *p-y* curves with pore pressure ratio variation at the depth of 1.5 m are combined and shown in Fig. 10. At low r_u, the *p-y* curves behaved almost linearly due to relatively constant soil stiffness and stress amplitude. As the excess pore pressure ratio increased, the secant modulus of the hysteretic loops decreased, and the areas of the loops increased, indicating that subgrade pressures have reduced and damping effects have increased. The evolution of dynamic *p-y* is the outcome of reduced soil stiffness and change of soil impedance.

Combining the results of coupled soil responses and dynamic *p-y* behavior revealed that soil stiffness variations due to pore pressure generation and induced strain level should be considered in dynamic *p-y* framework for liquefied sand. Also, the preliminary results proved that the testing configuration can capture major characteristics of pile-support wharf under kinematic and inertial excitations.

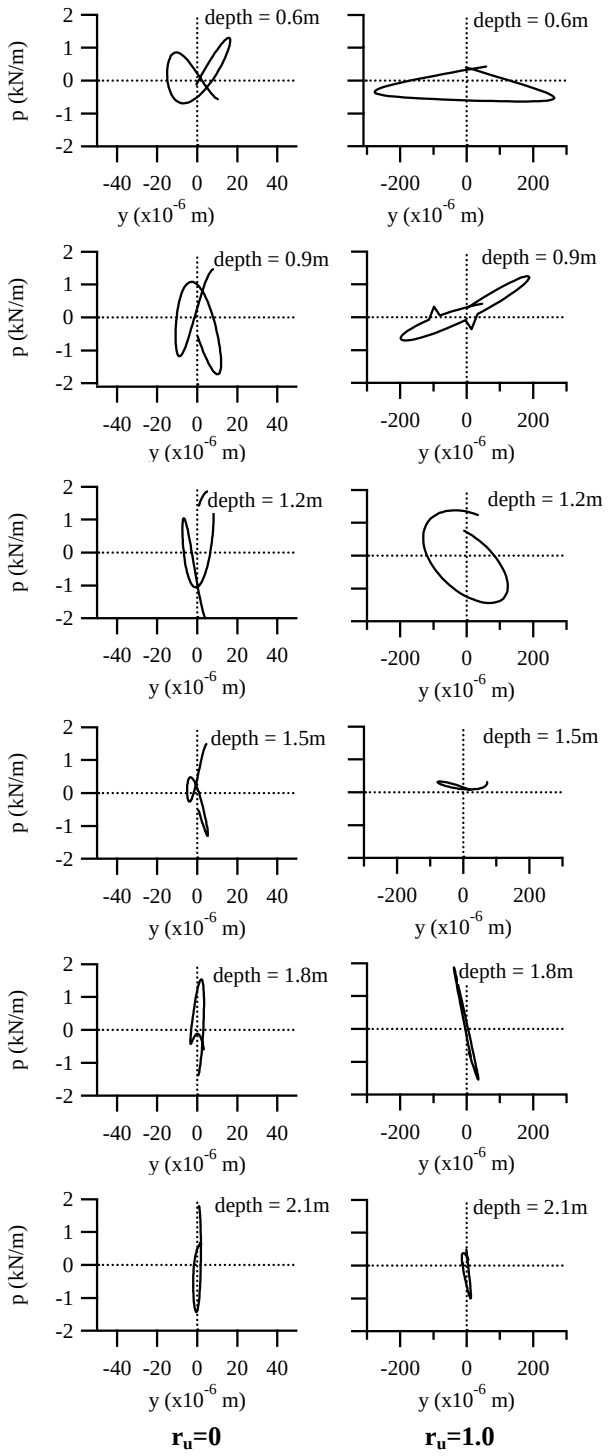

Fig. 9. Dynamic p-y response of Pile A at different r_u

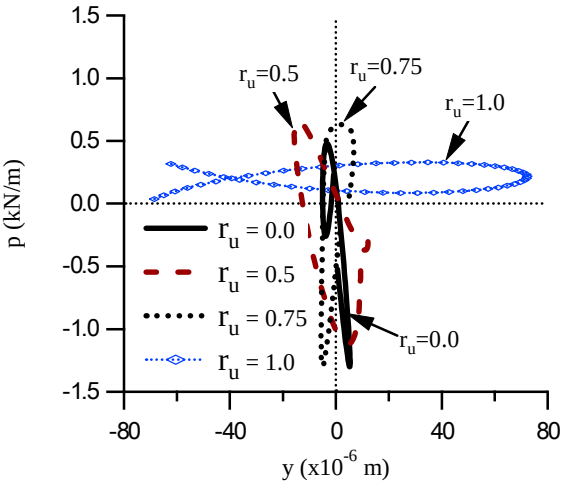

Fig. 10. Evolution of dynamic p-y response of Pile A

CONCLUSION

Field large-scale physical modeling using surface wave generator was performed to study dynamic soil-structure interactions in pile-supported wharf, verify configuration of an in situ monitoring station, and develop the technique for periodically checking of in situ instrumentation. Coupled shear strain-pore pressure generation behavior, pile responses, and soil-pile interaction characteristics were evaluated. Conclusions from preliminary results are drawn in what follows:

1. The testing results prove that the testing configuration and data reduction procedure can capture the interactions among the induced shear strain, generated excess pore pressure, and dynamic *p-y* behavior around piles.

2. Spatial variations of pore pressure histories show that the accumulation of excess pore pressure was affected by induced shear strain levels and pore pressure variations of nearby soil, and distance to the pile. The rate of excess pore pressure accumulation decreases as the distance to the pile increases.

3. Screening effect of horizontal stress waves not only affected the induced shear strain levels ahead and behind the pile but also created different loading mechanism for the second pile. The first pile was mainly subjected to kinematic forces from stress wave traveling through the soil and the second pile was subjected to inertial forces from forced displacement on pile head.

4. The dynamic *p-y* curves varies with variation of excess pore pressure of surrounding soil, which is the outcome of soil stiffness reduction and change of soil impedance on wave propagation. The testing results reveal that the

dynamic p-y concept should be modified for soil with significant excess pore pressure generation.

The performed test has following advantages. First, it can be performed in the field to evaluate seismic resistance of active wharf and to periodically check the integrity of in situ monitoring system. Second, the instrumentation configuration and data reduction procedure can be compared to real earthquake loading in terms of soil responses and soil-structure interactions. Third, the processed shear strains are directly related to engineering properties and rigorous in mechanics aspects. Finally, the pile responses due to kinematic and inertial effects can be studied in one testing configuration. The shortcomings include less screening effect in real seismic loadings, more sensors required for strain calculation, more complicated wave field than shaking table tests and real earthquake loadings, and scale and boundary effects on state of stress and wave fields that encounter in all model tests. Nevertheless, the proposed tests can be an alternative to current large-scale physical modeling and useful insights of soil-structure interaction can be obtained.

ACKNOWLEDGES

This study was supported by Harbor and Marine Technology Center, Institute of Transportation (IHMT), Taiwan, ROC, under contract No. MOTC-IOT-96-H1DB005. This support is gratefully acknowledged. The vibroseis was provided by CPC cooperation, Taiwan. Any opinions, findings, and conclusions or recommendations expressed in this material are those of the authors and do not necessarily reflect the views of the Institute of Transportation.

REFERENCES

Boulanger, R. W. Curras, C. J. Kutter, B. L. Wilson, D. W. and Abghari, A. [1999]. "Seismic Soil-Pile-Structure Interaction Experiments and Analyses," *Journal of Geotechnical and Geoenvironmental Engineering*, ASCE, Vol. 125, No. 9. pp.750-759.

Brandenberg, S.J. Boulanger, R.W. Kutter, B.L. Chang, D. [2005]. "Behavior of Pile Foundations in Laterally Spreading Ground during Centrifuge Tests", *Journal of Geotechnical and Geoenvironmental Engineering*, ASCE, Vol. 131, No. 11. pp. 1378-1391.

Chang, W. J. [2002]. "Development of an In Situ Dynamic Liquefaction Test," Ph.D. Dissertation, University of Texas at Austin.

Kamaji, N. Saito, H. Kusama, K. Kontani, O. and Nigbor R. [2004]. "Seismic Tests of a Pile-supported Structure in Liquefiable Sand Using Large-scale Blast Excitation," *Nuclear Engineering and Design*, Vol. 228, pp. 367-376.

Nakamura S. [1995]. *Applied Numerical Method in C*, Prentice Hall.

Rathje, E. M. Chang, W. J. and Stokoe, K. H. II [2005]. "Development of an In Situ Dynamic Liquefaction Test," *Geotechnical Testing Journal, ASTM*, Vol. 28, No. 1, pp. 65-76.

Rollins, K. M. Gerber, T. M. Lane, J. D. and Asford, S. A. [2005]. "Lateral Resistance of a Full-Scale Pile Group in Liquefied Sand," *Journal of Geotechnical and Geoenvironmental Engineering*, ASCE, Vol. 131, No. 1. pp.115-125.

Takahashi, A. and Takemura, J. [2005]. "Liquefaction-induced Large Displacement of Pile-supported Wharf," *Soil Dynamics and Earthquake Engineering*. Vol. 25, No.11, pp 811-825.

Tokimatsu, K. and Asaka, Y. [1998]. "Effects of Liquefaction-Induced Ground Displacements on Pile Performance in the 1995 Hyogoken-Nambu Earthquake," *Soils and Foundations*, Vol. 2, pp163–77.

Tokimatsu, K. and Suzuki, H., [2004]. "Pore Water Pressure Response around Pile and its Effects on p-y Behavior during Soil Liquefaction," *Soils and Foundations*, Vol. 44, No. 6, pp101–110.

Wang, S. T. and Reese, L. C. [1998]. "Design of Pile Foundations in Liquefied Soils,", *Proceedings of Geotechnical Earthquake Engineering and Soil Dynamics*, Seattle, Washington, pp. 1331-1343.

Werner, S. D. (ed.), [1998]. *Seismic Guidelines for Ports*. Technical Council on Lifeline Earthquake Engineering. Monograph No. 12. ASCE.

Woods, R. D., 1968, "Screening of Surface Waves in Soils," *Journal of the Soil Mechanics and Foundations Division*, ASCE, Vol. 94, No. SM4, pp. 951–979.